FINAL TECHNICAL REPORT

Department of Energy

Award FG02-96ER54360

"Topics in Plasma Physics"

Linda Vahala
Old Dominion University

1998 - 2013

1. Introduction

During the period 1998-2013, research under the auspices of the Department of Energy was performed on RF waves in plasmas. This research was performed in close collaboration with Josef Preinhaelter, Jakub Urban, Vladimir Fuchs, Pavol Pavlo and Frantisek Zacek (Czech Academy of Sciences), Martin Valovic and Vladimir Shevchenko (Culham).

RF plasma wave interactions with plasmas

A. Quasi-optical grill research [1-4]

The use of lower hybrid (LH) waves is considered very important for the control of current profiles in the outer plasma regions of tokamaks. This is especially true for the proposed ITER fusion device currently under construction in Cadarache, France. The design for the launch of high power LH waves in the 5-8 GHz range is difficult because of the required cooling of the launcher as well as structural stability since the grills are very narrow with thin walls separating the waveguides. One possible design for this standard multijunction grill is to consider the quasi-optical grill (QOG). The QOG is both a relatively simple design and gives robust performance. A pioneer of such a device is Preinhaelter. In particular, Preinhalter has suggested placing rods in an oversized waveguide (a hyperguide) and irradiate them obliquely by a wave emerging as a higher mode in an auxiliary oversized waveguide. The confining walls now become an intrinsic part of the structure, and one avoids mirrors and point-like sources. The reflected power can be handled by standard waveguide techniques.

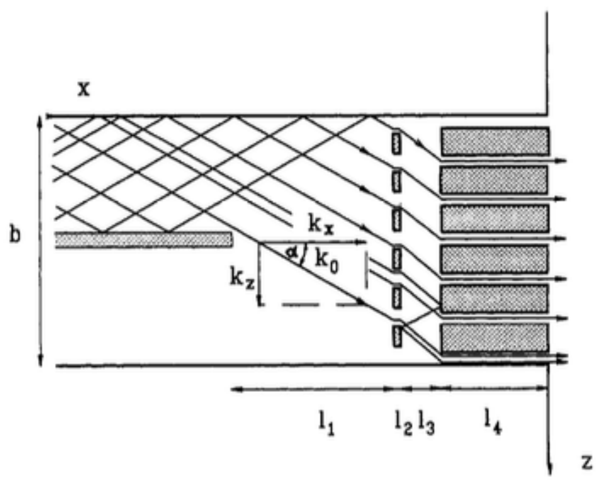

Fig. 1 A perpendicular cross section of the 2 rows of rods in the QOG, showing the ray trajectories in the auxiliary waveguide.

One of the first findings were that

(a) even though conducting walls surrounded the QOG, it does not prevent the rods from being proper irradiated,

(b) the resonant rod length ℓ_4, Fig. 1, in the main row of rods ensures a highly efficient structure, even when designed with just one row of rods.

(c) the overloading of the QOG is not that severe, and the **E**-field only becomes about 3 times higher than in the ideal case.

(d) the number of structure elements in the QOG are significantly less than those in the standard multijunction grill.

The weighted directivity for a QOG consisting of 2 rows of rods is shown in Fig. 2, while the spatial power spectrum from a QOG with 2 rows of 27 rods is given in Fig. 3.

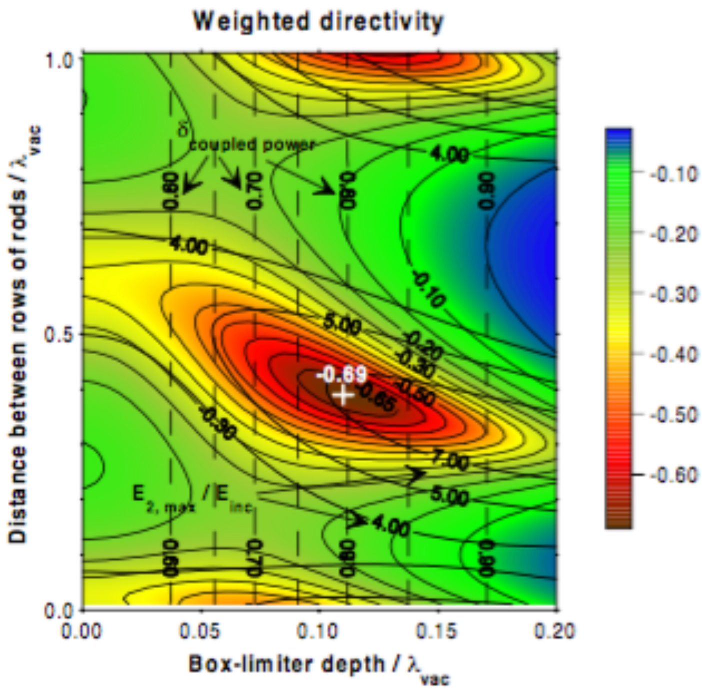

Fig. 2 The N_z-weighted directivity, with 2 rows of rods.

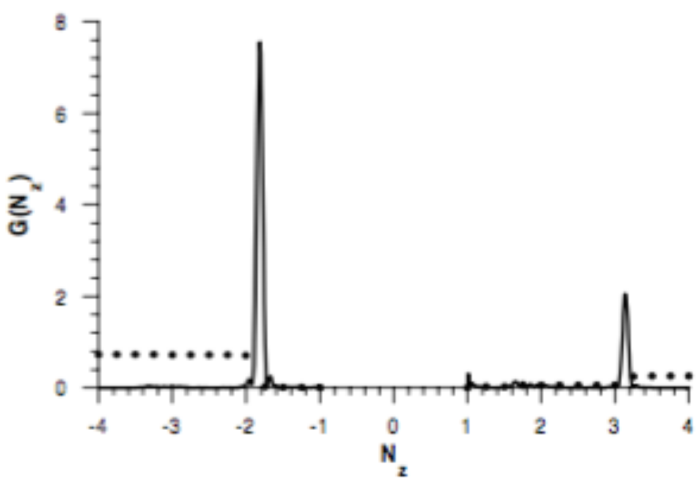

Fig. 3 The power spectrum from QOG from 2 rows of 27 rods.

There is currently a renewed interest in QOG antennas, and so we reconsidered the multijunction grill [5] and developed an efficient full wave code [*OLGA*] to study the coupling of the lower hybrid grill to the tokamak plasma. This code considers the full 3D geometry of the grill structure so as to efficiently determine the power density spectrum of the emitted waves, the wave reflection coefficient, the power lost by the waves that were launched into the inaccessible region as well as the directivity of the transmitted waves into the accessible region. *OLGA* can determine the 3D **E**-field in front of the grill. One theoretical difficulty is that there arises a very large number of 2D k-space infinite integrals that need to be evaluated for the coupling elements. The complexity of these integrals can be dramatically reduced by clever use of symmetry. High order Gaussian quadratures are employed together with 2D B-splines. *OLGA* can handle very large structures and many modes since the computational time is only weakly dependent on the size of the problem.

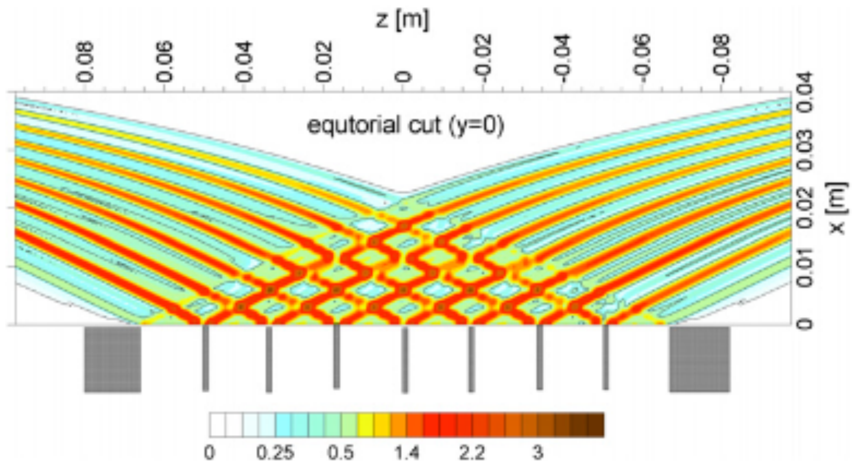

Fig. 4 Equatorial cross section of the Electric field just in front of an 8 waveguide grill (COMPASS plasma). $\left|E_z\left(x,0,z\right)\right|$ is shown in units of the incident TE_{10} amplitude.

Considerable research effort [6-19] has gone into the study of Electron Bernstein Waves (EBW) propagation in spherical tokamaks - like NSTX at Princeton and MAST (Culham). In these spherical tokamaks, the plasma is overdense because of lower toroidal magnetic fields. As a result of this overdenseness the standard launching of electron cyclotron (EC) transverse O- and X- modes fail to penetrate the plasma: the waves experience a cutoff and cannot penetrate into the plasma. Thus these EC waves cannot be used for either heating or current drive in spherical tokamaks. On the other hand, EBW are a quasi-electrostatic kinetic EC which can propagate and be strongly absorbed in an overdense plasma. But since the antenna emits electromagnetic waves we must have mode conversion in order to excite these electrostatic waves which cannot propagate in a vacuum. One thus requires the incident electromagnetic wave emitted from the antenna to be mode-converted within the plasma to an electrostatic wave. Preinhaelter, in 1973, promoted the O-X-B mode conversion process. The O-mode converts to a slow X-mode at the upper hybrid resonance (UHR). This occurs near the plasma edge (actually the O-mode is first converted to the fast branch of the X-mode which propagates towards higher density where it smoothly converts to the slow X-mode branch. This then propagates back towards the edge of the plasma towards to the upper hybrid resonance). This then converts to the EBW. An alternate mode conversion scheme is the XB scheme: but this scheme is typically efficient for lower frequencies and requires specific density scale lengths. On the other hand, the OXB scheme is more universal in terms of frequency and density length scales. In Fig. 5 we plot the radial profiles in the midplane of the characteristic frequencies for various NSTX and MAST plasmas. The simulated frequency ranges are shown shaded and these bound the EBW propagation regions from the UHR at the plasma edge to the cold EC resonance. The plasma is overdense and the first three EC harmonics are inaccessible- and X- modes in NSTX and MAST $\left(\omega_{pe} > n\omega_{ce}\right)$. We consider the first two EC harmonics as we expect the higher harmonics will be overlapping due to Doppler broadening.

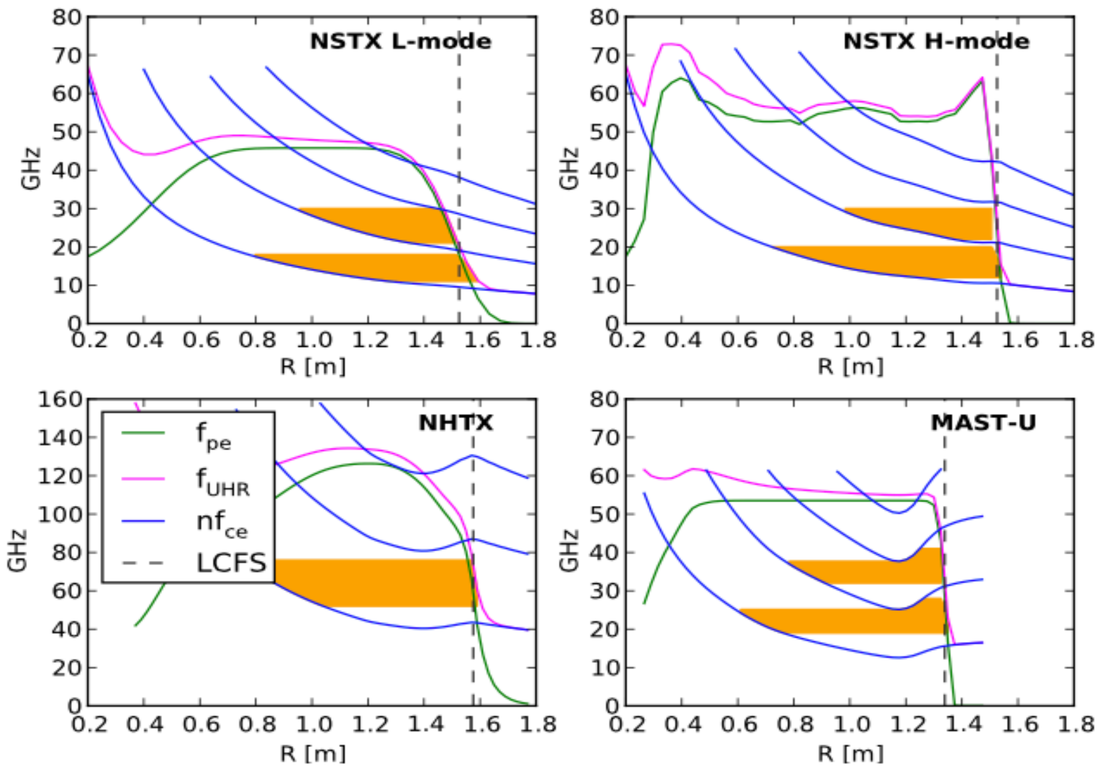

Fig. 5 The accessible frequencies for EBW propagation in various spherical plasma experiments. The dashed vertical is the last closed flux surface (LCFS).

In Fig. 6 we consider the effect of 2 different vertical launch positions for an NSTX L-mode plasma, using 17 GHz on the ray trajectories and the evolution of $N_{||}$

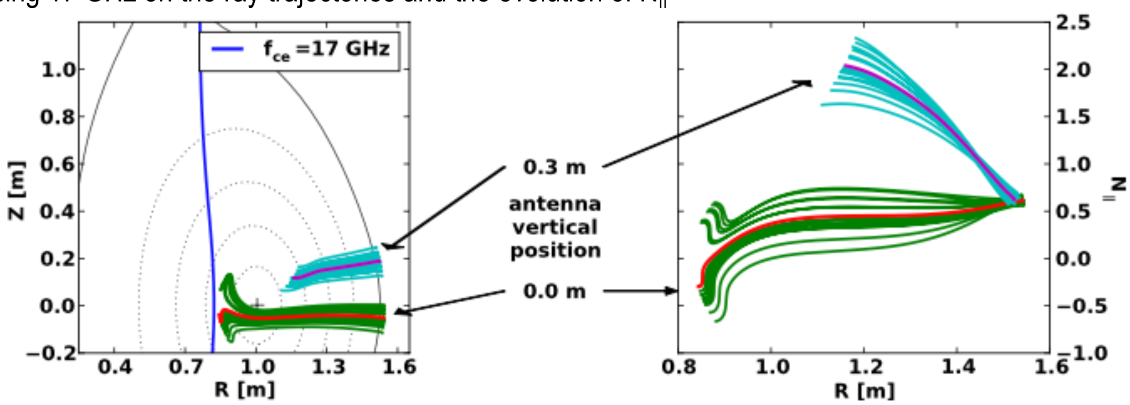

Fig. 6 Ray trajectories and the evolution of $N_{||}$ for NSTX L-plasmas at 17 GHz from 2 different launch positions: 0, and 0.3 m.

Those rays that are launched close the midplane propagate straight to the magnetic axis, and the central ray's $N_{||}$ do not change appreciably until the ray approaches resonance (around R = 1 m). Now $|N_{||}|$ will start to increase exponentially and the beam splits into two parts that propagate vertically in opposite directions. The rays are finally absorbed. For off-midplane launch the wave $|N_{||}|$ steadily increases and the waves are absorbed at the Doppler-broadened EC resonance. In this case, since all the $N_{||}$ now have the same sign, one achieves high current drive efficiency.

4. Qubit unitary lattice algorithms for the Nonlinear Schrodinger equation [20-38]

Quantum entanglement is the vine from which the branches of the fields of quantum computing and quantum information theory spring using qubits as their building blocks. Unlike the classical binary bit, which can take on the value of "0" or "1", the qubit state exists as a superposition of these classical states "0" and "1". In particular the qubit $|q\rangle$

$$|q\rangle = \gamma_0|0\rangle + \gamma_1|1\rangle \quad , \text{ with } |\gamma_0|^2 + |\gamma_1|^2$$

where γ_0 and γ_1 are complex probability amplitudes. For quantum entanglement we must entangle at least two qubits

$$|q_1 q_2\rangle = \gamma_{00}|00\rangle + \gamma_{01}|01\rangle + \gamma_{10}|10\rangle + \gamma_{11}|11\rangle \quad , \text{ with } |\gamma_{00}|^2 + |\gamma_{01}|^2 + |\gamma_{10}|^2 + |\gamma_{11}|^2 = 1$$

While the more traditional approach to quantum dynamics is through the Hamiltonian or Lagrangian, Feynman first introduced the approach of qubit dynamics. An important advantage of these qubit representations is that they are close to ideally parallelized (since their structure is a collide-sequence on a lattice, similar to its non-unitary cousin lattice Boltzmann) and can be encoded onto a quantum computer.

The quantum lattice gas (QLG) is one of the earliest unitary algorithms that is based on an interleaved sequence of unitary collide-stream operators on qubit probability amplitudes. Again this is a mesoscopic representation, and in the Chapman-Enskog limit one desires to recover the nonlinear physics equations under consideration. Since the QLG is a mesoscopic perturbative approach, the algorithm must be benchmarked. We present here some benchmarking on the inelastic vector soliton collisions, governed by the coupled (1D) nonlinear Schrodinger equations:

$$i\frac{\partial Q_1}{\partial t} = -\frac{\partial^2 Q_1}{\partial x^2} - 2\mu\left(|Q_1|^2 + B|Q_2|^2\right) Q_1$$

$$i\frac{\partial Q_2}{\partial t} = -\frac{\partial^2 Q_2}{\partial x^2} - 2\mu\left(|Q_2|^2 + B|Q_1|^2\right) Q_2$$

for the electric field polarization amplitudes for single mode propagation in an optical birefringent medium. B is the cross phase birefringence modulation coefficient. Interestingly, these equations also show up for the mean field approximation of Bose-Einstein condensates at T = 0.

For these Manakov solitons there are some initial vector soliton amplitudes which will result in an inelastic collision: one of the soliton post-collision amplitudes will be zero. This is not possible in scalar soliton collisions since we have the normalization constraints

$$\int dx \left|Q_i\left(x,t\right)\right|^2 = c_i = (\text{constant})_i \ , \ i = 1 \ , \ 2$$

This type of inelastic collision fuels the thought that these inelastic Manakov solitons can be used for digital information processing in a nonlinear optical medium without radiation losses.

In QLG, the unitary mesoscopic lattice algorithm with interleaved collision-stream operators: the unitary collision operator locally entangles the qubit amplitudes while the unitary stream operators transport that entanglement throughout the spatial lattice. The local unitary collision operator is that determined by Yepez in his work on QLG for the 3D relativistic Dirac particle dynamics, and then extended it by adding an effective potential as a Lorentz mass scalar:

$$C_{D,j} = \begin{pmatrix} \cos\theta_j(x) & -i\sin\theta_j(x) \\ -i\sin\theta_j(x) & \cos\theta_j(x) \end{pmatrix} \quad , \quad \theta_j(x) = \frac{\pi}{4} - \frac{1}{8}\Omega_j^2(x) \ , \ j = 1,2$$

where the nonlinear interaction terms

$$\Omega_1(x) = 2\mu\left(\left|Q_1(x)\right|^2 + B\left|Q_2(x)\right|^2\right) \quad , \quad \Omega_1(x) = 2\mu\left(\left|Q_1(x)\right|^2 + B\left|Q_2(x)\right|^2\right)$$

The unitary streaming operator, though written in terms of the Pauli spin matrices, is just a shift operator, where $S_{\Delta x,j}$ is that shift by $\Delta x = \pm 1$. With the interleaved non-commuting stream-collide sequence

$$I_{xj} = S_{-\Delta x,j} C \, S_{\Delta x,j} C$$

one can then define the unitary evolution operator.

An inelastic Manikov vector soliton is shown in Fig. 7

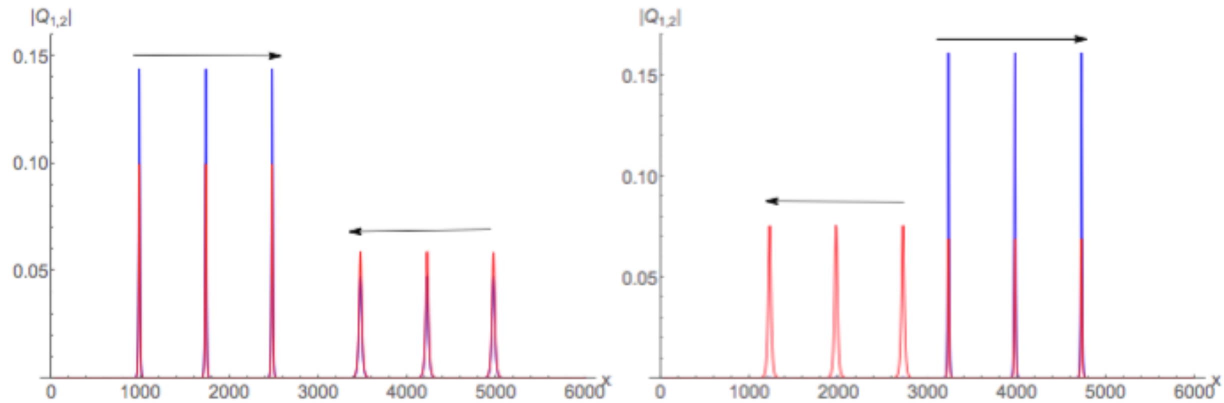

(a) pre-collision solitons *(b) inelastic post-collision solitons*

Fig. 7 The pre-collision states (a) at t = 0, 10k, 20k, with the post-collision states (b) at t = 25k, 35k, 45k. The $|Q_1|$ polarization is in blue, while the $|Q_2|$ polarization is in red. For the specially chosen initial amplitudes, one of the $|Q_1|$ -post collision solitons is eliminated

A plot of the soliton peaks is shown in Fig. 8. There is only inelastic collision – the first collision – since the requirements on the collision amplitudes are very stringent. There is a quasi-inelastic collision around time step 280k.

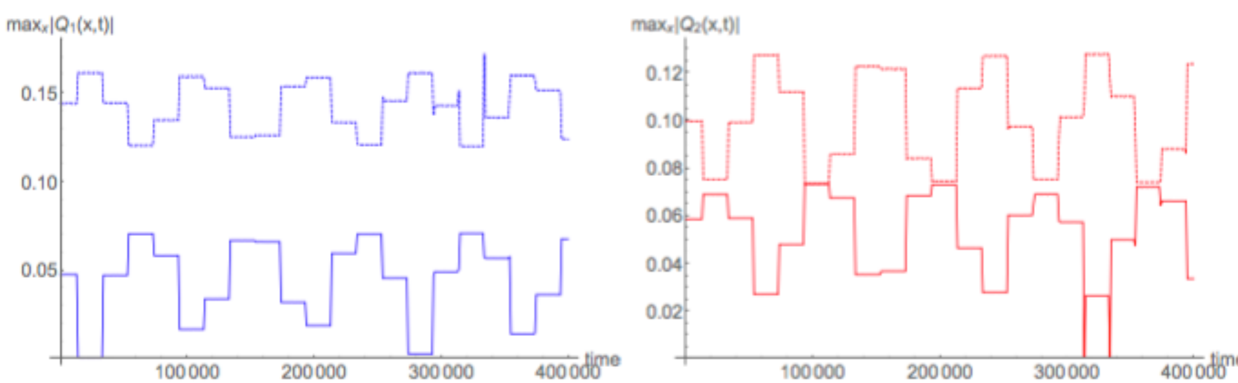

Fig. 8 The plot of the maxima amplitudes of the polarization solitons.

It is important that the maximum stable amplitude that can be run in QLG with the Dirac-based collision operator is an order of magnitude greater than that from the square-root-of-swap collision operator.

PAPERS PUBLISHED/PRESENTED DURING 1998-2013 PERIOD

[1] "Proposals of Quasi-Optical Grill for ITER Tokamak"
J. Preinhaelter, M. Z. Irzak, A. Cote, L. Vahala and G. Vahala
25th EPS Conference on Control Fusion and Plasma Physics
Prague, Czech Republic, Vol. 22C, p. 1426-1429 (1998) (ed. P. Pavlo).

[2] "Quasi-Optical Grill Structures for TdeV, Ignitor and Tore Supra Tokamaks"
J. Preinhaelter, M. A. Irzak, A. Cote, Y. Demers, V. Fuchs, L. Vahala and G. Vahala
2nd Eurepean Topical Conference on RF Heating and CDE of Fusion Devices
Brussels, Belgium, p. 145 (1998)

[3] "Proposals of quasi-Optical Grills for ITER and NSTX Tokamaks"
J. Preinhaelter, M. A. Irzak, L. Vahala and G. Vahala
26th EPS Conference on Controlled Fusion & Plasma Physics, Maastricht, 1999
ECA 23J, p. 1601-1604, editors: Schweer, van Oost, Vietzke

[4] "Quasi-Optical Grills for ITER and NSTX Plasmas"
J. Preinhaelter, M. A. Irzak, L. Vahala and G. Vahala
AIP Conference Proceedings #485, p. 474-477 (1999), editors: Bernabei & Paoletti

[5] "An analysis of lower hybrid grill coupling using an efficient full wave code",
J. Preinhaelter, J. Urban, L. Vahala and G. Vahala,
Nucl. Fusion 52, 083005 (2012)

[6] "Excitation of Electron Bernstein Waves in MAST"
J. Preinhaelter, F. Zacek, P. Pavlo, L. Vahala and G. Vahala
27th EPS Conference in Control, Fusion and Plasma Physics, eds. K. Szego, T. N. Todd, S. Zoletnik, (Budapest, Hungary, 12-16 June 2000), p. 402

[7] "ECRH in Spherical Plasmas: O-X-EBW Mode Conversion in MAST"
J. Preinhaelter, M. A. Irzak, L. Vahala, G. Vahala,
Rev. Sci. Instrum. 72, 391 (2001).

[8] "ECE on CASTOR"
J. Preinhaelter, M. A. Irzak, E. Tregubova, L Vahala, G. Vahala and F. Zacek
Radio Freq. Power in Plasmas, AIP #595 (ed. Mau and deGrassie), p. 326 (2001).

[9] "Influence of the Plasma Surface Density Fluctuations on ECE in CASTOR"
J. Preinhaelter, J. Stockel, F. Zacek, M. A. Irzak, E. Tregubova, L. Vahala and G. Vahala
28th EPS Conference in Control. Fusion and Plasma Physics
(Maidera, Portugal, June 2001).

[10] "Interpretation of ECE Measurements on MAST"
J. Preinhaelter, V. Shevchenko, M. Valovic, P. Pavlo, L. Vahala, G. Vahala Proc. 29th
EPS Conference on Controlled Fusion and Plasma Physics Montreux, Switzerland,
ECA 26B, P-5.095 (2002)

[11] "Electron Bernstein Wave-X-O Mode Conversion and Electron Cyclotron Emission in MAST"
J. Preinhaelter, P. Pavlo, V. Shevchenko, M. Valovic, MAST Team, L. Vahala and
G. Vahala
Rev. Sci. Instrum. 74, 1437-1440 (2003)

[12] "ECE in MAST: theory and experiment"
J. Preinhaelter, V. Schevchenko, M. Valovic, P. Pavlo, L. Vahala, G. Vahala, and the MAST team
Radio Frequency Power in Plasmas, AIP Conference Proc. 694, 388-391 (2003)

[13] "Influence of Antenna Directivity on ECE in MAST"
J. Preinhaelter, V. Schevchenko, J. Urban, M. Valovic, P. Pavlo, L. Vahala, G. Vahala, and MAST team
Rev. Sci. Instrum. 75, 3804-3806 (2004)

[14] "The Sensitivity of ECE simulations in MAST to Different Magnetic Equilibria Models"
J. Preinhaelter, V. Shevchenko, M. Valovic, H.R. Wilson, J. Urban, P. Pavlo, L. Vahala, G. Vahala, and MAST team
31st European Phys. Soc. Conf. On Plasma Physics, ECA Vol. 28G, P-4, 184 (2004)

[15] "EBW Simulation for MAST AND NSTX Experiments"
J. Preinhaelter, G. Taylor, V. Shechenko, J. Urban, M. Valovic, P. Pavlo, L. Vahala and
G. Vahala
AIP Conf. Proc. 787, 349-352 (2005)

[16] "Methodology of Electron Bernstein Wave Emission Simulations"
J. Urban, J. Preinhaelter, V. Schevchenko, G. Taylor, M. Valovic, P. Pavlo, L. Vahala, and
G. Vahala
32nd European Phys. Soc. Con. On Plasma Physics, ECA Vol.29G, P1.121 (Tarragona Spain), 2005

[17] "Electron Bernstein Wave Simulations and Comparison to Preliminary NSTX Emission Data"
J. Preinhaelter, J. Urban, P. Pavlo, G. Taylor, V.Shevchenko, M. Valovic, L. Vahala and G. Vahala
Rev Sci. Instrum 77, 10F524 (2006)

[18] "EBW power deposition and current drive in WEGA – comparison of simulation with experiment",
J. Preinhaelter, H. P. Laqua, J. Urban, L. Vahala and G. Vahala, Plasma Phys. Control. Fusion 51, 125008 (2009)

[19] , "A survey of electron Bernstein wave heating and current drive potential for spherical tokamaks",
J. Urban, J. Decker, Y. Peysson, J. Preinhaelter, V. Shevchenko, G. Taylor, L. Vahala and G. Vahala
Nucl. Fusion 51, 083050 (2011)

[20] "Quantum Lattice Gas Representation of Some Classical Solitons"
G. Vahala, J. Yepez and L. Vahala
Phys. Lett. A310, 187-196 (2003)

[21] "Lattice Boltzmann and Quantum Lattice Gas Representation of One-Dimensional m Magnetohydrodynamic Turbulence
L. Vahala, G. Vahala and J. Yepez
Phys Lett. A306, 227-234 (2003)

[22] "Quantum lattice gas representation for vector solitons"
G. Vahala, L. Vahala, and J. Yepez
SPIE Conf. Proc. 5105, 273-281 (2003)

[23] "Inelastic Vector Soliton Collisions: A Quantum Lattice Gas Representation"
G. Vahala, L. Vahala and J. Yepez
Phi. Trans. Roy. Soc. London 362, 1677-1690 (2004)

[24] "Quantum lattice gas representation of dark solitons"
G. Vahala, L. Vahala and J Yepez
SPIE Conf. Proc. 5436, 376-385 (2004)

[25] "Quantum Lattice Representation of 1D MHD turbulence with arbitrary Transport Coefficients"
J. Yepez, G. Vahala and L. Vahala
SPIE Conf. Proc. 5815, 227-235 (2005)

[26] "Scientific Visualization as Part of the Computational Model Development Process"
S. Ziegeler, G. Vahala, L. Vahala, and J. Yepez
NAVO Navigator, p. 19-23, (2005)

[27] "Quantum Lattice Representations for Vector Solitons in External Potentials"
G. Vahala, L. Vahala an J. Yepez
Physcia A362, 215-221 (2006)

[28] "Lattice Quantum Algorithm for the Schrodinger Wave Equation in 2+1 Dimensions with a Demonstration by Modeling Soliton Instabilities"
J. Yepez, G. Vahala and L. Vahala
Quantum Info. Process. 4, 457-469 (Dec 2005)

[29] "Quantum Lattice Gas Algorithm for Quantum Turbulence and Vortex Reconnection in the Gross- Pitaevskii Equation"
G. Vahala, J. Yepez and L. Vahala, , Proc. SPIE, 6976, 69760U1-10 (2008)

[30] "Vortex-antivortex pair in a Bose-Einstein condensate, J. Yepez, G. Vahala and L. Vahala, Eur. Phys. J. Special Topics 171, 9-14 (2009)

[31] "Superfluid Turbulence from Quantum Kelvin Wave to Classical Kolmogorov Cascades", J. Yepez, G. Vahala, L. Vahala and M. Soe, Phys. Rev. Lett. 103, 084501 (2009)

[32] "Unitary quantum lattice gas representation for 2D quantum turbulence", B. Zhang, G. Vahala, L. Vahala, M. Soe, Proc. SPIE 8057, 80570E1-12 (2011)

[33] "Unitary quantum lattice algorithm for two-dimensional quantum turbulence", B. Zhang, G. Vahala, L. Vahala, M. Soe, Phys. Rev. E84, 046701 (2011)

[34] "Poincare recurrence and spectral cascades in three-dimensional quantum turbulence", G. Vahala, J. Yepez, L. Vahala, M. Soe, B. Zhang and S. Ziegeler Phys. Rev. E84, 046713 (2011)

[35] "Unitary qubit lattice simulations of multiscale phenomena in quantum turbulence", M. Soe, G. Vahala, L. Vahala and J. Yepez. Supercomputing 2011, paper TCC304, Nov. 2011 (Seattle)

[36] "Qubit lattice (QLG) simulations for a T > 0 superfluid", G. Vahala, B. Zhang, L. Vahala, M. Soe and S. Ziegeler DoD High Performance Computing, User Group Conference, 2011

[37] "Unitary Qubit Lattice Gas Representation of 2D and 3D Quantum Turbulence", G. Vahala, B. Zhang, J. Yepez, L. Vahala and M. Soe, Chpt. 11 (pp. 239 - 272), in *Advanced Fluid Dynamics,* ed. H. W. Oh, (InTech Publishers, Croatia, 2012)

[38] "Unitary qubit lattice simulations of complex vortex structures", G.Vahala, J. Yepez, L. Vahala and M. Soe, Computat. Sci & Discovery, 5, 014013 (2012)